Project Report Entitled

"Theoretical and Numerical Study of Air Flow Through Single Hole Orifice meter"

In Fulfillment of Course Project Requirement

ME 724

Submitted by

Aayush Patel (183109002)

Vaibhav Jaiswal (18310R002)

Under the Guidance of

Prof. Abhilash J. Chandy

Department of Mechanical Engineering

Indian Institute of Technology Bombay

Powai – 400 076, Maharashtra, India

June 2020

Contents

List of figures iii
Introduction 1
Applications 2
Motivation and impact of studying the problem 2
Objective 2
Literature Review 3
Modelling of Turbulent Flow 11
Modeling of equations in LES: 11
Conclusion 13
References 13

List of figures

Figure 1 Schematic diagram of orifice meter 1
Figure 2 Dimensionless (A) centerline axial velocity and (B) wall pressure profiles for air (Re=91,100), CFD simulations (—), Experimental data of Morrison (□) [2] 5
Figure 3 Radial profiles of axial velocity at various axial locations. (1) z=40, (2) z=40.1, (3) z=40.2, (4) z=40.3, (5) z=40.4, (6) z=40.45. (A) Radial profiles of axial velocity at various axial locations close to downstream of the orifice meter. (1) z1=40.25,(2) z1=40.26 (3) z1= 40.27 (4) z1= 40.28 (5) z1= 40.29 (6) z1=40.30. [2] 5
Figure 4 Radial profiles of turbulent kinetic energy (k) at various axial locations. (1) z=40, (2) z=40.05, (3) z=40.2, (4) z=40.35, (5) z=40.4, (6) z=40.45. (B) Radial profiles of turbulent kinetic energy (k) at various axial locations close to downstream of orifice meter. (1) z=40.25, (2) z=40.255, (3) z=40.26, (4) z=40.265, (5) z=40.27, (6) z=40.275, (7) z=40.28, (8) z=40.285, (9) z=40.29, (10) z=40.295, (11) z=40.3. [2] 6
Figure 5 (A) Radial profiles of turbulent dissipation rate (e) at various axial locations. (1) z=40, (2) z=40.05, (3) z=40.2, (4) z=40.35, (5) z=40.4, (6) z=40.45. (B) Radial profiles of turbulent dissipation rate (e) at various axial locations close to downstream of orifice meter.(1) z=40.25, (2) z=40.255, (3) z=40.26, (4) z=40.265, (5) z=40.27, (6) z=40.275, (7) z=40.28, (8) z=40.285, (9) z=40.29, (10) z=40.295, (11) z=40.3. [2] 6
Figure 6 Variation in flow rate with square root of pressure drop across orifice meter. Experiment with flange taps (●), CFD prediction with vena-contracta taps (■) [2] 7
Figure 7 Scaled axial velocity variance [3] 8
Figure 8 Scaled Radial velocity variance [3] 8
Figure 9 Scaled Azimuthal velocity variance [3] 9
Figure 10 Scaled axial-radial velocity covariance 9
Figure 11 Axial-azimuthal velocity covariance 10
Figure 12 Scaled axial-azimuthal velocity covariance 10
Figure 13 Turbulent kinetic energy [3] 10

Introduction

There are many methods to measure the flow rate. One of the methods is direct method simply measuring the amount of fluid that accumulates in a container over a fixed period of time. Another method is positive displacement flow meter example includes household water and gas meter. There is another method which is called restriction flow meter. The details of this method are as follows:

The principle of restriction flow meter is that change in velocity leads to change in pressure. This pressure change is measures by a pressure gauge or manometer. By applying modified Bernoulli equation and continuity equation we can prove that the mass flow rate is proportional to the square root of pressure difference. The devices which come under this category are flow nozzle, venturi meter and orifice plate. These devices have different geometries.

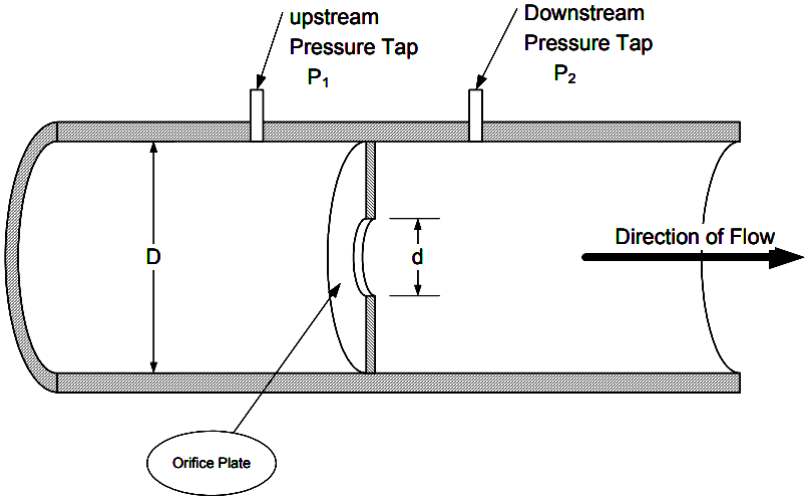

Figure 1 Schematic diagram of orifice meter

Orifice meter is a widely used measurement device in industrial application because of its simplicity and low installation cost. Orifice Meter contains a thin hole plate that is mounted between pipe flanges. This literature carries the analysis of flow through an orifice meter. since most of the flows are in the range of high Reynolds number .so it is important to inderstand characteristic of turbulent flow.

Turbulent flow [1] is characterized by eddies with a wide range of length and time scales. The largest eddies are typically comparable in size to the characteristic length of the mean flow. The

smallest scales are responsible for the dissipation of turbulence kinetic energy. The brief summary of turbulent

- Momentum, mass, energy and other scalars are transported mostly by large eddies.
- Large eddies are dependent on the geometries and Boundary conditions of flow involved
- Small eddies are less dependent on geometry and tend to be more isotropic in nature.

Applications

It is used to measure the flow rates of the fluid in single state (i.e gaseous state or liquid state) or mixed state (both gaseous and liquid state).Examples of industrial applications are like water treatment plants, gas industries, refineries, petrochemical plants etc.

Motivation and impact of studying the problem

Orifice meter is supplied with discharge coefficient and installation procedure. Discharge coefficient is defined as the ratio of actual flow to the theoretical flow. It is obtained by means of experiments. So, to reduce cost of experiments the computer simulations are carried out to find discharge coefficients for various flow rates and beta ratios. CFD simulations are useful to find discharge coefficients but also, they are used to find out flow patterns and exact location of vena-contracta as it varies with Reynolds number and beta ratio (orifice diameter/pipe diameter).

So, in closure of the problem CFD analysis of orifice meter helps to find out modification of current orifice meter.

Objective

The objective of the work is to understand the underlying concept of turbulent flows

- turbulent air flow through an obstruction.
- Velocity profile and pressure distribution at various axial upstream and downstream of orifice.
- Variance and covariance of velocity component as a measure of velocity fluctuation and shear stress.
- Turbulent kinetic energy production and dissipation.
- Methods of turbulent modelling.

Literature Review

There are many experimental and numerical results in this topic which is listed in Table- 1. Nail (1991) has presented experimental measurements of centerline axial velocities, wall static pressure, Reynold's stresses and wall shear stresses measured using LDA (Laser Doppler Anemometer). Morrison also used LDA and reported mean velocity and turbulence field inside orifice flow meter with a beta ratio of 0.5. Centerline axial velocity and wall pressure profiles were also presented.The below table shows the brief overview of the literature being made.

Author	Pipe diameter (mm)	β	Working fluid	Range of *Re*	Remarks
Ho and Leung (1985)	25.4	0.247, 0.36, 0.448	water	100–1000	Low *Re* (laminar flow) experiments. Variation in C_D vs. *Re* presented.
Nail (1991)	25.4	0.5	air	18,400	Experiments using 3 Dimensional LDA technique.
Morrison et al. (1993)	50.8	0.5	air	91,100	Experiments using 3 Dimensional LDA technique. Measured mean velocity and wall pressure. Turbulence quantities calculated and discussed in detail.
Smith et al. (2008)	25.4	0.5, 0.6, 0.8	air	18,400	Effect of turbulence models (k–ε and RSM) on mean axial velocity and wall pressure studied using CFD simulation and compared with experimental data of Nail.
Naveenji et al. (2010)	50, 100, 200	0.4–0.8	Non-Newtonian fluids (prepared with varying concentration of salt)	100–10,000	C_D vs. *Re* predicted using CFD simulation.
Oliveira et al. (2010)	100	0.1–0.6	water	4000–10^6	Predicted pressure drop vs. flow rate with various values of β, C_D vs. *Re* and wall pressure using CFD simulation.

The details of two literature is given below

1)Manish S. Shah *et al.* [2] investigated the behavior of fluid in orifice meter numerically and experimentally, by varying the beta ratio (0.12 to .9) and Reynolds number (4500 to 20000). They used the k-e model for numerical simulation and validated them with experimental results. The aim was to find out discharge coefficients (Cd). In addition to this they found out location of vena contracta and showed mechanism to locate vena contracta in actual orifice meter. They performed grid independent study to find out the mesh size that was sufficiently fine so that the solution does not change by further refining the mesh. The details of mesh refinement are given below. figure table no.3

Case no.	fluid	Orifice dimensions					Remarks
		Pipe diameter (mm)	β	L_U (mm)	L_T (mm)	t (mm)	
1	Water	12.3	0.4065	246	494	2	Experiments are conducted in the present study. Coarse mesh—321,360 cells Fine mesh—10,47,360 cells
2	Water	12.3	0.162	246	494	2	Mesh used—49,695 hexahedra cells
3	Water	12.3	0.081	246	494	2	Mesh used—12,13,950 hexahedra cells
4	Air	25.4	0.5	500	1200	3.75	Experimental data of Morrison et al. (1993) used for comparison Mesh used—283,700 hexahedra cells
5	Air	50.8	0.5	50.8	228.6	3.2	Experimental data of Nail (1991) used for comparison Mesh used—112,700 hexahedra cells

Governing equation, boundary condition for the flow and the k-e model. All the details are given below in the table. In all the simulations, velocity is set at the inlet of the orifice meter, pressure is set at the outlet and no-slip condition is set at the wall. The k-e model is having additional boundary condition: Turbulent intensity =5%. The formulation of turbulent kinetic energy is given below figures and equation for dissipation rate is given below.

$$I_T = \left(\frac{\sqrt{k}}{v_{avg}}\right)$$

$$k = I_T^2 u_{avg}^2$$

$$\varepsilon = \frac{k^{3/2}}{6\left(\left(\frac{1}{20}\right)D\right)}$$

Which gives

$$\varepsilon = \frac{k^{\frac{3}{2}}}{0.3D}$$

$$\varepsilon = C_\mu^{\frac{3}{2}} \frac{k^{\frac{3}{2}}}{l}$$

$$l = (0.09)^{3/4} \frac{k^{3/2}}{\varepsilon} = 0.16 \frac{k^{3/2}}{\varepsilon}$$

By rearranging we get

$$\varepsilon \cong \frac{k^{3/2}}{6l}$$

i)Velocity profile: They plotted radial velocity profile at different axial locations mainly orifice upstream and downstream which is shown below in two separate figures. They also plotted normalized pressure at different locations. location of vena contracta is location of maximum velocity. Firstly, it was validated against Morrison data and it shows excellent agreement.

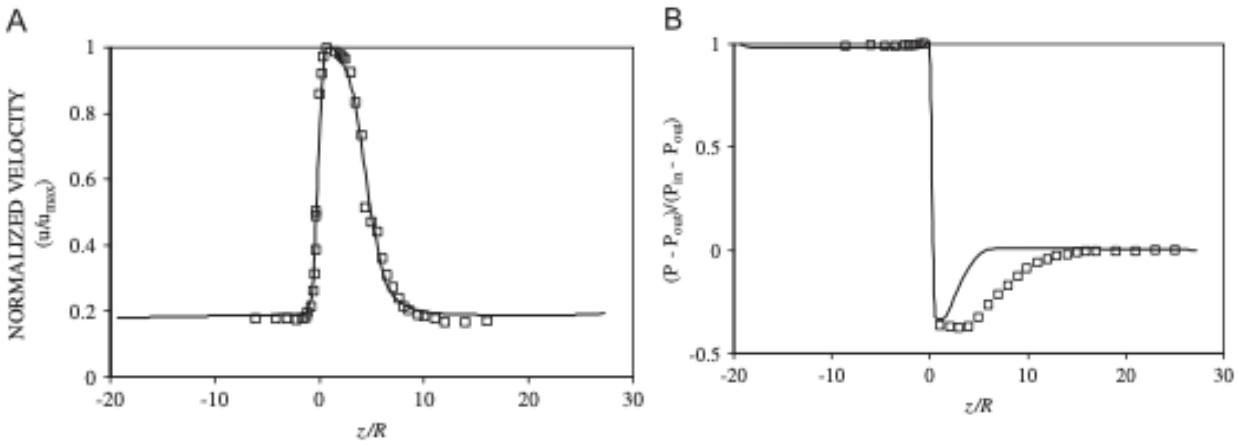

Figure 2 Dimensionless (A) centerline axial velocity and (B) wall pressure profiles for air (Re=91,100), CFD simulations (—), Experimental data of Morrison (□) [2]

Results of radial velocity profile at various location upstream and downstream are plotted in the figure below in part A and part B respectively.

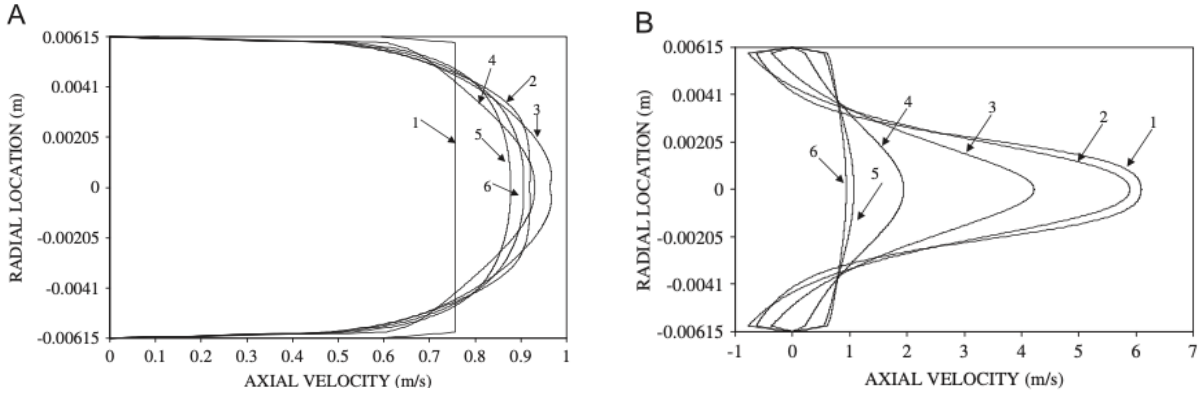

Figure 3 Radial profiles of axial velocity at various axial locations. (1) z=40, (2) z=40.1, (3) z=40.2, (4) z=40.3, (5) z=40.4, (6) z=40.45. (A) Radial profiles of axial velocity at various axial locations close to downstream of the orifice meter. (1) z1=40.25,(2) z1=40.26 (3) z1= 40.27 (4) z1= 40.28 (5) z1= 40.29 (6) z1=40.30. [2]

ii) k-e profiles: The plots are given below. form the graph we can conclude that both energies have higher value near to wall in the fully developed upstream and downstream turbulent region because of higher velocity gradients. In the region just after orifice, highest velocity gradients are expected at the orifice wall which forms due to flow separation.

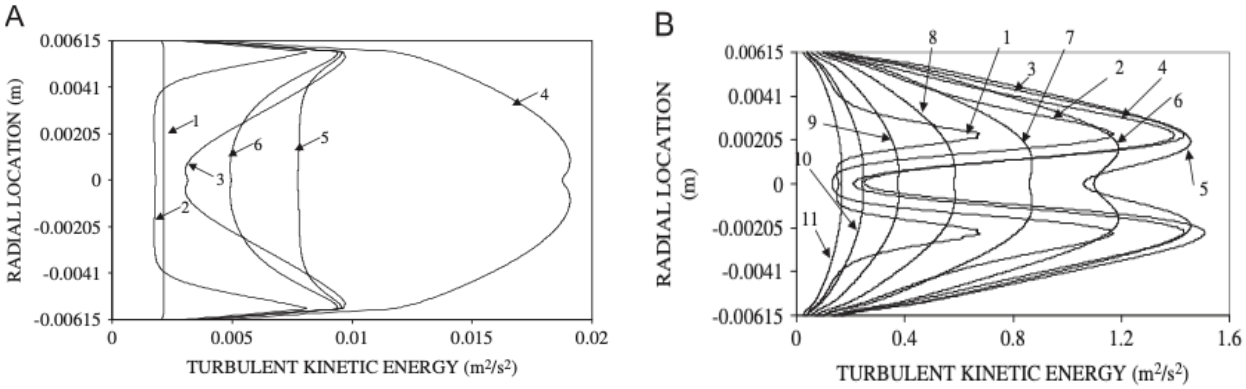

Figure 4 Radial profiles of turbulent kinetic energy (k) at various axial locations. (1) z=40, (2) z=40.05, (3) z=40.2, (4) z=40.35, (5) z=40.4, (6) z=40.45. (B) Radial profiles of turbulent kinetic energy (k) at various axial locations close to downstream of orifice meter. (1) z=40.25, (2) z=40.255, (3) z=40.26, (4) z=40.265, (5) z=40.27, (6) z=40.275, (7) z=40.28, (8) z=40.285, (9) z=40.29, (10) z=40.295, (11) z=40.3. [2]

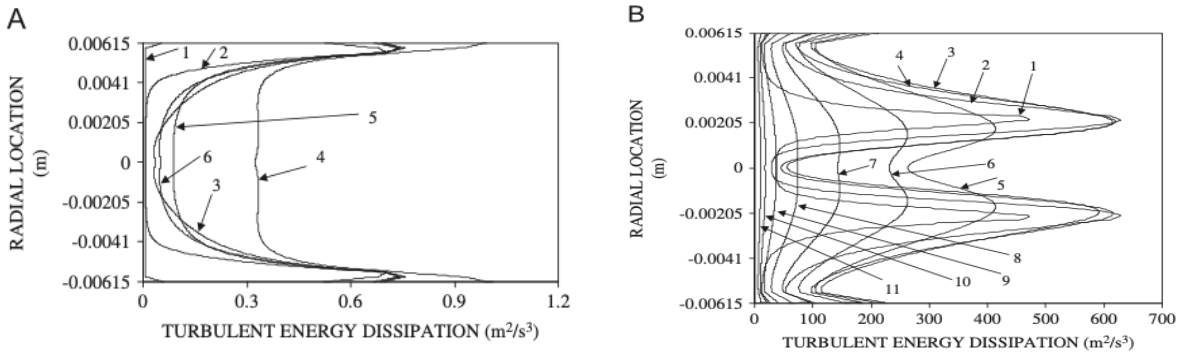

Figure 5 (A) Radial profiles of turbulent dissipation rate (e) at various axial locations. (1) z=40, (2) z=40.05, (3) z=40.2, (4) z=40.35, (5) z=40.4, (6) z=40.45. (B) Radial profiles of turbulent dissipation rate (e) at various axial locations close to downstream of orifice meter.(1) z=40.25, (2) z=40.255, (3) z=40.26, (4) z=40.265, (5) z=40.27, (6) z=40.275, (7) z=40.28, (8) z=40.285, (9) z=40.29, (10) z=40.295, (11) z=40.3. [2]

iii) Results of discharge coefficient both numerical and experimental by varying the flow rates are given below. It gives good agreement with experimental data.

Details of experiments conducted with water as fluid and the values of orifice coefficient.

Sr. no.	Q (ml/s)	ΔP (N/m^2)	Inlet velocity (ms^{-1})	Velocity at throat (ms^{-1})	Pipe *Re*	Discharge coefficient	
	(measured)	(measured with flanged taps)	(calculated)	(calculated)	(calculated)	Experimental	CFD simulation
1	44.67	5680.08	0.376	2.275	4489	0.6657	0.6253
2	57.33	10,866.24	0.482	2.920	5762	0.6177	0.6128
3	80	23,461.20	0.673	4.074	8040	0.5866	0.6035
4	89.67	29,511.72	0.755	4.567	9012	0.5863	0.5996

iv) To get the validation of theoretical formulation of flow rate with pressure drop, they plotted the graph of flow rate against square root of pressure drop. The graph is linear and it seems to be an excellent validation as you can see from the figure.

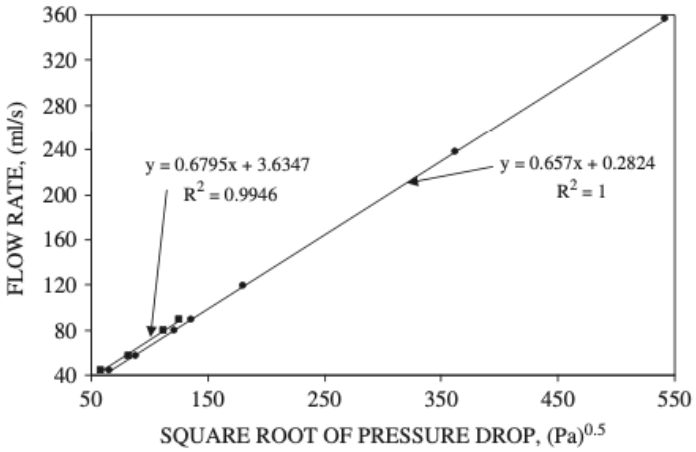

Figure 6 Variation in flow rate with square root of pressure drop across orifice meter. Experiment with flange taps (●), CFD prediction with vena-contracta taps (■) [2]

2) Gerald L. Morrison *et al.* [3] has carried out experimental study of the mean velocity and turbulence fields inside a $\beta = 0.5$ orifice flowmeter. 3-D LDA system with argon -ion laser is used to supply three colours: 476, 488, and 514.5nm. Each color measuring an independent velocity component. Measurement of velocity were done at 700 locations with 4096 measurements at each location. Velocity profile upstream of the obstruction followed the typical power law of the turbulent flows. At $X/R = -1.13$, the fluid particles started to gain radial velocity while moving towards the obstruction. To accommodate increased mass flow from the radial direction, the centerline velocity of particle increases as it approaches orifice. Centerline velocity further increases until vena contracta and then velocity decreases on further downstream motion. The location of vena contracta is at 0.75R downstream and minimum pressure occur at 1.5R. the location of minimum pressure is downstream of the maximum velocity because of two-dimensional nature of the pressure field. The recirculating downstream of orifice produces both axial and radial variation in velocity and hence a radially varying pressure field.

3-D LDV technique is useful for calculation of complete Reynolds stress tensor. Additional terms are introduced in momentum equation by Reynolds decomposition and time averaging process. IN 3-D incompressible flow Reynolds stress is a tensor with 6 independent and a total of nine components. The terms along the diagonal statistically represents variance of instantaneous

velocity components, while off-diagonal elements represent covariances. The diagonal components are incorporated alongside the normal stresses while diagonal elements as shear stresses in RANS equation. The contours for normal variance for each velocity component is shown in figure. Significant increase in the normal variance is observed just downstream of the orifice plate which suggests the existence of steep mean velocity gradient in the area. The region of increasing variance peaks within the shear layer and gradually decreases as flow progresses downstream. Recirculating eddies downstream of the orifice causes radial momentum transfer between high speed centerline velocity and relatively low velocity recirculating flow near the walls. The decrease in local time averaged velocity gradient reduces energy input to the eddies resulting in decay of eddies and hence the turbulence level. At the same time there is no change in variance upstream. The variance in radial and axial directions are around 50 percent of velocity in respective direction and therefore shows anisotropic nature of turbulent flow.

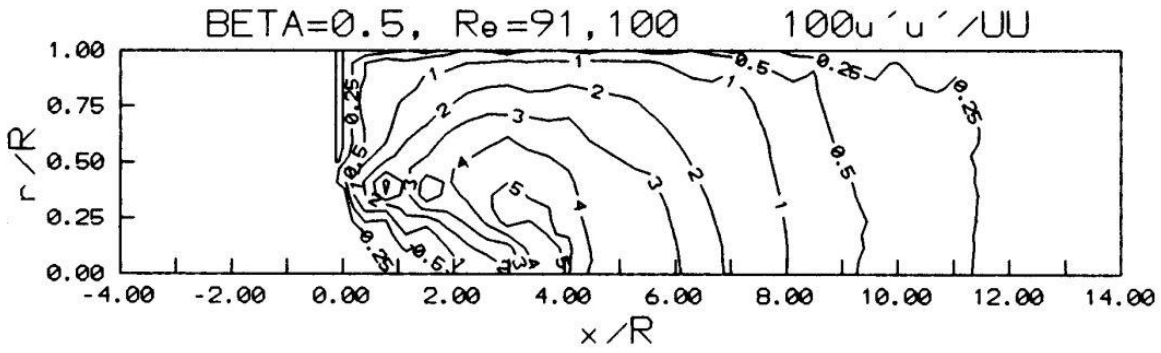

Figure 7 Scaled axial velocity variance [3]

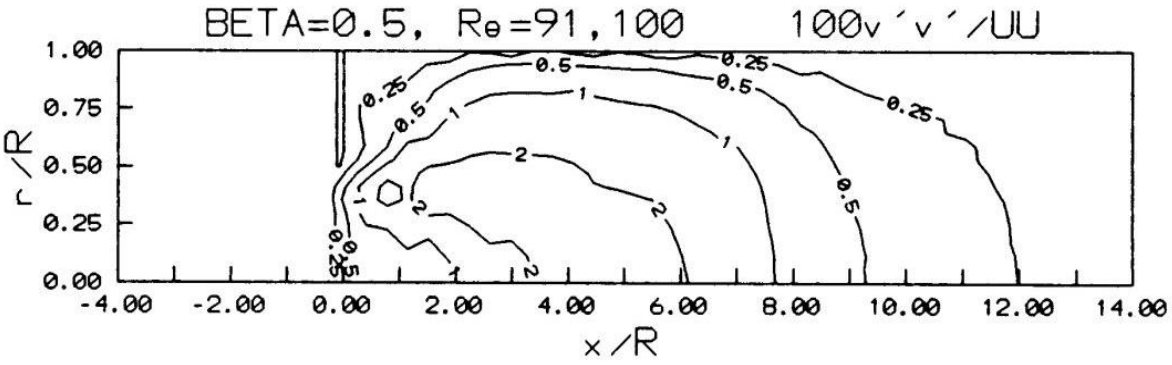

Figure 8 Scaled Radial velocity variance [3]

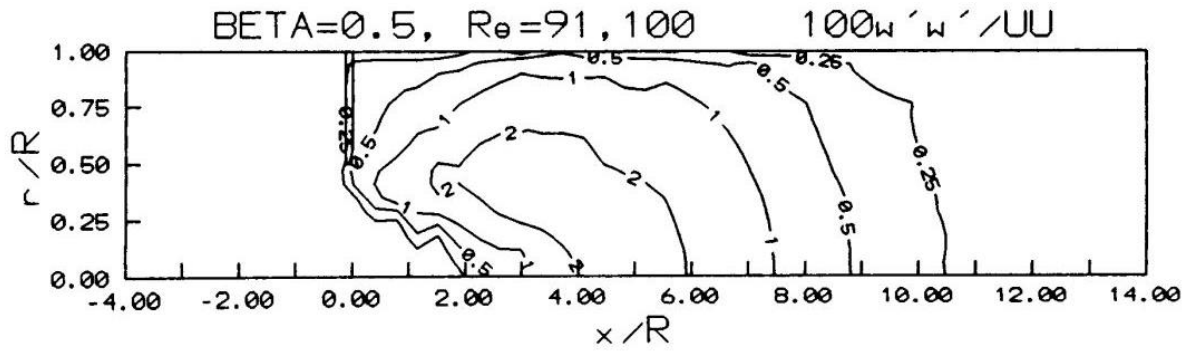

Figure 9 Scaled Azimuthal velocity variance [3]

Contour plots (fig. 10,11,12) shows distribution of covariance terms or the shear stress terms. These terms are measure of momentum exchange between respective velocity components. The order of axial-radial term is much higher than other terms which signifies its larger contribution towards momentum exchange. Axial-radial covariance can also be thought of as measure of radial transfer of axial momentum, eddies at the recirculating zone ejects high speed jet momentum and also ingest low speed recirculation fluid into the jets. Higher magnitude of radial-axial covariance term as compared to radial-azimuthal and axial-azimuthal suggest negligible transfer of momentum to azimuthal direction. The axial radial orientation of shear layer causes higher axial radial covariance term.

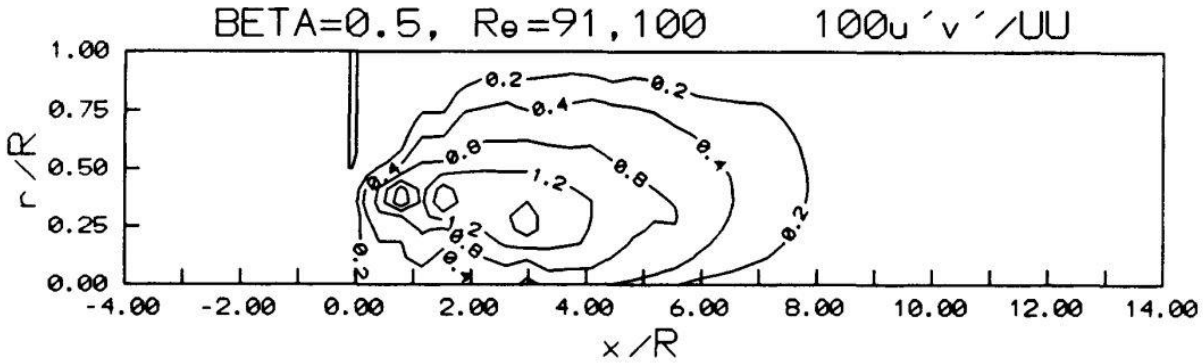

Figure 10 Scaled axial-radial velocity covariance

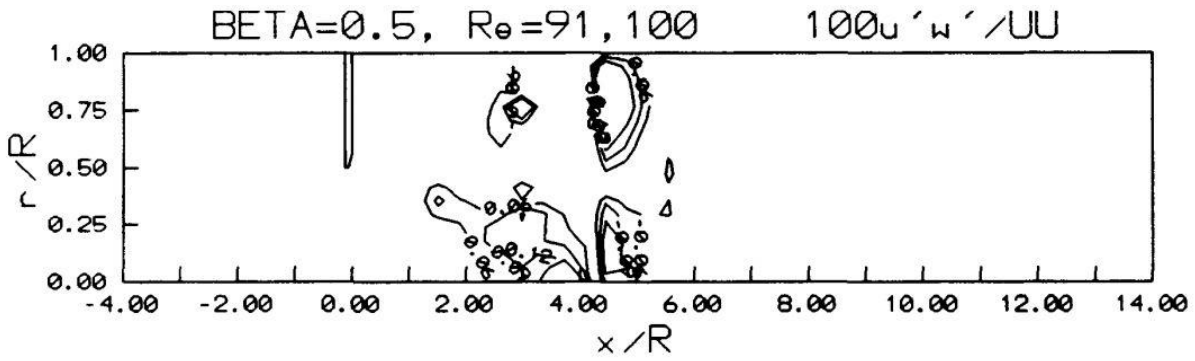

Figure 11 Axial-azimuthal velocity covariance

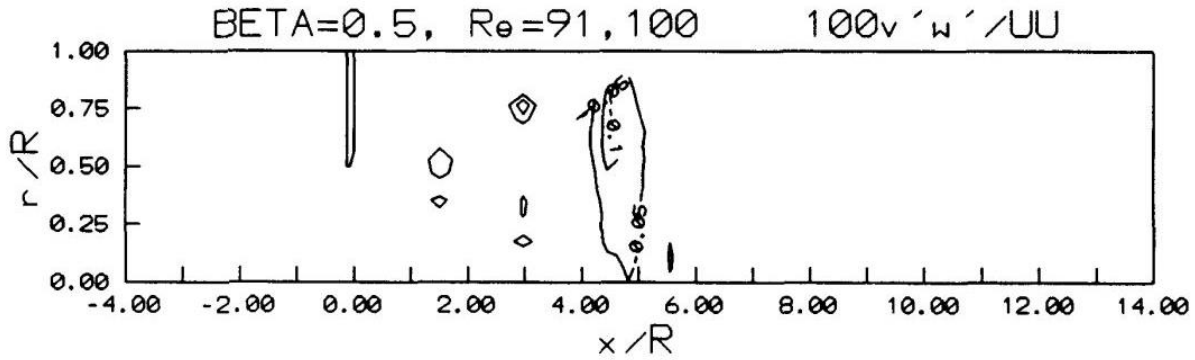

Figure 12 Scaled axial-azimuthal velocity covariance

A rise in turbulent kinetic energy is observed just downstream of the orifice plate. Spread of the contour downstream of peaks shows gradual dissipation of turbulent kinetic energy as flow happens. The plots of turbulent kinetic energy is similar to individual variance of components, and also variation of axial-radial component is similar to turbulent kinetic energy.

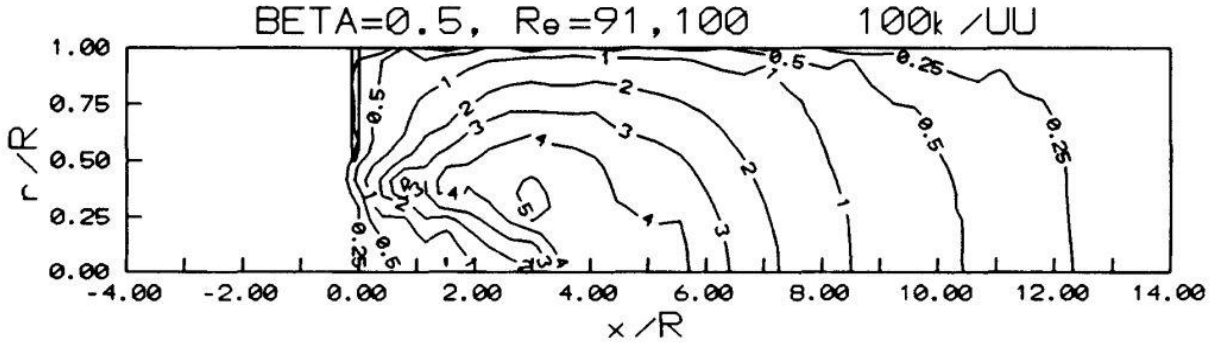

Figure 13 Turbulent kinetic energy [3]

Modelling of Turbulent Flow

In most of the purposes, orifice meter operates in high Reynolds number range. So in this problem turbulent effects have to be introduced in the CFD simulations.

There are many approaches to solve turbulent flows like

1) Simple k-e model

2) k-e model with SST

3) LES model

4) DNS model

The literature available for orifice meter used k-e model for simulating the flow in the orifice meter. So here we want to simulate above problem using LES model.

Overview of LES

- LES [4] is a transient turbulence model that falls midway between RANS and DNS models
- Its main advantage is improved accuracy compared to RANS models
- It needs coarser mesh and larger times step sizes in LES than in DNS.LES still requires substantially finer meshes than those typically used for RANS calculations
- LES has to be rum for a sufficiently long flow time to obtain stable statistics of flow being modeled. As a result, the computational cost involved with LES is normally orders of magnitudes higher than that for steady RANS calculations in terms of CPU time.
- Furthermore, storage and analysis of the large data sets that are generated is a significant practical problem

Modeling of equations in LES:

- The governing equations employed for LES are obtained by filtering the time -dependent Navier-Stokes equations in either Fourier (wave number) space or configuration (physical) space. The filtering process effectively filters out the eddies whose scale are smaller than filter width or grid spacing used in the computation. The resulting equations thus govern the dynamics of large eddies.
- A filtered variable (denoted by an overbar) is defined by

$$\overline{\emptyset} = \int \emptyset(x')G(x,x')dx'$$

- The finite volume discretization itself implicitly provides the filtering operation

$$\overline{\emptyset}(x) = \frac{1}{V}\int \emptyset(x')dx', \quad x' \in v$$

- Where V is the volume of a computational cell. The filter function $G(x,x')$ implied as follows

$$G(x,x') = \begin{cases} \frac{1}{V}, & x' \in v \\ 0, & x'otherwise \end{cases}$$

- Filtering the Navier-Stokes equations, the following results obtain

$$\frac{\partial \rho}{\partial t} + \frac{\partial}{\partial x_i}(\rho \overline{u_\iota}) = 0$$

Where term below is the stress tensor due to molecular viscosity defined by

$$\sigma_{ij} \equiv \mu\left(\frac{\partial \overline{u_\iota}}{\partial x_j} + \frac{\partial \overline{u_j}}{\partial x_i})\right] - \frac{2}{3}\mu\frac{\partial \overline{u_\iota}}{\partial x_j}\delta_{ij}$$

$$\frac{\partial}{\partial t}(\rho \overline{u_\iota}) + \frac{\partial}{\partial x_j}\left(\rho \overline{u_\iota}\overline{u_j}\right) = \frac{\partial}{\partial x_j}\left(\sigma_{ij}\right) - \frac{\partial \bar{p}}{\partial x_i} - \frac{\partial \tau_{ij}}{\partial x_i}$$

The term below is sub grid-scale stress defined by

$$\tau_{ij} \equiv \rho\overline{u_\iota u_J} - \rho\overline{u_\iota}\overline{u_J}$$

Conclusion

In this report we have discussed about turbulent flow in obstruction type flowmeter. Focus of this project work is to understand turbulent flow characteristics with the help of single hole orifice meter. We have gone through numerical as well as experimental literature concerning single hole orifice meters. CFD predictions for flow pattern, pressure recovery and velocity profiles are in line with the experimental results. CFD techniques are very cost effective and efficient technique in terms of designing and understanding the flow through such a geometry. In addition to its applicability of standard k-e turbulence model for capturing turbulence effect in orifice flow is well attributed.

References

[1] P. J. Pritchard, "Introduction to fluid Mechanics".

[2] M. S. Shah, J. B. Joshi, A. S. Kalsi, C. Prasad and D. S. Shukla, "Analysis of flow through an orifice meter: CFD simulations," *Chemical Engineering Science,* pp. 300-309, 2012.

[3] G. L. Morrison, R. D. Jr., G. Nail and D. Panak, "Mean velocity and turbulence fields inside a b1⁄40.50 orifice flowmete," *AIChE,* pp. 745-756, 1993.

[4] "LES (large eddy simulation) ANSYS theory guide 12.0".

[5] G. Nail, "A study of 3-Dimensional flow through orifice meters, Ph.D. Dissertation, Texas A&M University, USA.".

[6] A. Naveenji, S. Malavarayan, M. Kaushik and H. Sriananth, "CFD analysis on discharge coefficient during non-Newtonian flows through orifice meter.," *International Journal of Engineering Science and Technology,* 2010.